FISEVIER

Contents lists available at ScienceDirect

Developmental and Comparative Immunology

journal homepage: www.elsevier.com/locate/devcompimm



HSC70 functions as a negatively regulator in IFN signaling pathway via suppressing K63-linked ubiquitination of RIG-I in black carp

Jiaxin Fu ^{a,1}, Nianfeng chen ^{a,1}, Tian Qin ^a, Yixin Chen ^a, Ji Liu ^a, Hui Wu ^a, Jun Yan ^{a,*}, Jun Xiao ^{a,b,**}, Jun Zou ^c, Hao Feng ^{a,b}

ARTICLE INFO

Keywords: Black carp RIG-I HSC70 Ubiquitination Innate immunity

ABSTRACT

Heat shock cognate 70 (HSC70), a highly conserved molecular chaperone in the heat shock protein 70 (HSP70) family, plays an essential role in maintaining the homeostasis of the cellular environment. Furthermore, although previous studies have investigated potential function of HSC70 in innate antiviral immunity, further research is still required to fully elucidate its role. In this study, we cloned and characterized the HSC70 homolog gene from black carp (Mylopharyngodon piceus), which consists of 1950 nucleotides encoding 650 amino acids, migrates at approximately 71 kDa on SDS-PAGE, and is distributed in the cytoplasm. In response to different stimuli (SVCV, poly (I:C) and LPS), the transcription level of black carp HSC70 (bcHSC70) all increased to a certain extent. Luciferase reporter assay demonstrated that co-transfected bcHSC70 obviously reduced activity of interferon (IFN) promoters mediated by most factors in the RLRs pathway, and further qRT-PCR and plaque assay indicated that co-transfection of bcHSC70 with bcRIG-I decreased the bcRIG-I-mediated IFN transcription and antiviral ability resisting spring viremia of carp virus (SVCV), whereas knockdown of bcHSC70 improves the host cellular antiviral activity. Noteworthily, co-immunoprecipitation (co-IP) assay and immunofluorescence (IF) assay confirmed bcHSC70 interacts with bcRIG-I, and weaken K63-linked polyubiquitination of bcRIG-I. In summary, our study revealed that HSC70 negatively regulates IFN signaling pathway through impairing K63-linked ubiquitination of RIG-I in black carp, which provides an important basis for exploring innate immune regulatory mechanisms in teleost fish.

1. Introduction

Vertebrates rely on both innate and adaptive immunity to resist pathogenic microorganisms. However, the lower vertebrate primarily rely on innate immunity to defend against various detrimental microorganisms rather than adaptive immunity (Gomes et al., 2020). Innate immunity is the primary immune barrier against the invasion of viruses, which covered the important process that the pattern recognition receptors (PRRs) recognizing pathogen-associated molecular patterns (PAMPs) and inducing a range of antiviral immune responses. Classically, PRRs encompass toll-like receptors (TLRs), nod-like receptors

(NLRs), c-type lectin receptors, cytosolic DNA sensors, as well as retinoic acid-inducible gene-I-like receptors (RLRs) (Freed et al., 2014; Gong et al., 2019). RLRs consist of retinoic acid-inducible gene protein I (RIG-I), melanoma differentiation associated gene 5 (MDA5), and laboratory of genetics and physiology 2 (LGP2), and RLR signaling pathway is a key signaling pathway in the innate immune system against RNA viruses (Liao et al., 2021). Once the host is invaded by RNA virus, RIG-I and MDA5 immediately recognize it and activate the downstream mitochondrial antiviral signaling protein (MAVS). Subsequently, activated MAVS further recruits TANK-binding kinase 1 (TBK1), IkB kinase ε (IKK ε), then phosphorylates IFN regulatory factor 3/7 (IRF3/7) and

a State Key Laboratory of Developmental Biology of Freshwater Fish, College of Life Science, Hunan Normal University, Changsha, 410081, China

^b Institute of Interdisciplinary Studies, Hunan Normal University, Changsha, 410081, China

c Key Laboratory of Exploration and Utilization of Aquatic Genetic Resources, Ministry of Education, Shanghai Ocean University, Shanghai, 201306, China

^{*} Corresponding author. state key laboratory of developmental biology of freshwater fish, college of life science, Hunan Normal University, Changsha, 410081, China.

^{**} Corresponding author. state key laboratory of developmental biology of freshwater fish, college of life science, Hunan Normal University, Changsha, 410081, China.

E-mail addresses: yj1214@hunnu.edu.cn (J. Yan), xiaojun@hunnu.edu.cn (J. Xiao).

 $^{^{1}\,}$ These authors contributed equally to this paper.

nuclear factor κB inhibitor protein (NF- κB), ultimately inducing the type I IFN production and other antiviral proteins to eliminate viral infection (Solstad et al., 2022).

RIG-I as a crucial sensor for detecting the invasion of RNA viruses, possessing a DExD/H-box Helicase domain, a repressor domain (RD), and two caspase recruitment domains (CARDs) (He et al., 2023; Leung et al., 2012). When RIG-I detects pathogen RNAs, and then undergoes conformational changes, firmly anchoring the virus within its receptor and activating downstream signaling molecules, ultimately inducing the production of type I IFN to combat the viral infection (Kowalinski et al., 2011; Thoresen et al., 2021). RIG-I deficiency significantly impairs the host innate immunity to resist pathogenic microorganisms (Yang et al., 2021), while overactivation of RIG-I will lead to the autoimmune diseases (Kato et al., 2015). Therefore, strict regulation of RIG-I activity is essential for the host to resist invasion of viruses and maintain immune homeostasis. Moreover, in teleost fish, RLR signaling pathway also plays an important role in the innate immune response, such as recently studies have reported that zebrafish RIG-I could significantly induce the expression of IRF7, IFN and Mx, thereby confer resistance to SVCV infection (Zou et al., 2015). In black carp, RIG-I exists in two isoforms: RIG-Ia and RIG-Ib. Interestingly, only RIG-Ib activates IFN expression and has antiviral activity, not RIG-Ia (Liu et al., 2023). Besides, the RIG-I activation is tightly regulated by multiple molecules in teleost fish. For example, zebrafish TRIM25 and RNF135 could positively regulate the RLR/IFN signaling pathway via promoting the K63-linked ubiquitination of RIG-I (Jin et al., 2019; Lai et al., 2019). However, the research on the negative regulatory mechanism of RIG-I in fish is still limited.

Heat shock proteins (HSPs) are part of the cellular molecular chaperone system, which are widely distributed in microorganisms and mammalian cells. There are seven major families of HSPs, namely HSP110, HSP100, HSP90, HSP70, HSP60, HSP40, and small HSPs (approximately 15-30 kDa) (Tutar et al., 2010), which protected cells from a variety of physical and chemical stressors, such as temperature changes, ultraviolet radiation and pathogen invasion (Zininga et al., 2018). Heat shock cognate 70 (HSC70, as known as HSPA8) (Stricher et al., 2013), as a member of the HSP70 family, exhibits high homology in all species and plays essential roles in protein quality control, such as regulating misfolding and translocation of proteins, and targeting proteins for degradation by lysosomal or ubiquitin-proteasome pathway (Wang et al., 2020). In addition, previous studies have reported that HSC70 was involved in innate and adaptive host immunity, such as HSC70 participated in virus-induced adaptive immune responses by presenting antigenic peptides to CD4+T cells via MHC-II and acting as a regulator of autophagy (Bonam et al., 2019), and HSC70 negatively regulated VSV-induced antiviral response by restraining MAVS aggregation (Liu et al., 2013). In teleost fish, it has been reported that HSC70 blocked hormone-induced apoptosis in whole blood preparations from silver sea bream, and zebrafish HSC70 could degrade SVCV G protein via MARCH8-mediated lysosomal pathway, thereby inhibiting SVCV replication (Li et al., 2021). However, the regulatory mechanism of HSC70 in RLR/IFN signaling is still unclear in teleost fish.

In this study, our results revealed that heat shock cognate 70 (HSC70) reducing the level of K63-linked polyubiquitination of RIG-I for the first time, leading to suppression of cellular antiviral response in black carp. These findings provide important data to elucidate the regulatory mechanism of RLR/IFN signaling in the innate immunity in black carp.

2. Materials and methods

2.1. Cells, plasmids, and reagents

HEK293T, HeLa, *Epithelioma papulosum* cyprinid (EPC) and *Mylopharyngodon piceus* kidney (MPK) cells were maintained in the lab (Yang et al., 2024). Among them, HEK293T and HeLa cells were cultured at 37 °C, while EPC and MPK cells were cultured at 28 °C; all of them were

maintained with 5% CO2.

pcDNA5/FRT/TO-bcRIG-I-Flag, pcDNA5/FRT/TO-HA-Ub/ K63O/K48O, pcDNA5/FRT/TO-Myc-Ub, Luci-bcIFNα, Luci-DrIFNφ1, Luci-epcIFN (for black carp, zebrafish, EPC IFN promoter activity analysis respectively), and pRL-TK were kept in the lab. The recombinant expression plasmids HA-bcHSC70 and bcHSC70-Myc were constructed by inserting the open reading frame (ORF) of bcHSC70 into pcDNA5/ FRT/TO-HA-N or pcDNA5/FRT/TO-C-Myc, respectively. The knockdown plasmids targeting bcHSC70 were constructed by inserting shRNAs into pLKO.1. The related primers were designed on the GPP Web (https://portals.broadinstitute.org/gpp/public/seq/search). All the primer sequences were referenced in Table 1. The transfection reagents were Polyethylenimine (PEI) (Yeasen, China) and LipoMax (Sudgen, China) and the antibodies and agarose beads related to immunoblotting (IB) are as follows: Mouse monoclonal anti-HA antibody (Sigma, USA), mouse anti-Flag (Sigma, USA), mouse monoclonal anti-Myc antibody (Affinity), mouse monoclonal anti-β-actin antibody (Abcam, UK), mouse anti-Flag conjugated protein A/G agarose beads (Sigma, USA), and mouse anti-HA conjugated protein A/G agarose beads (Sigma, USA), These were used according to the manufacturers' instructions.

2.2. Virus infection, titer detection and virus production

The spring viremia of carp virus (SVCV/strain: SVCV741) was kept in our lab. For virus infection, EPC cells were infected with SVCV at different multiplicity of infections (MOIs) in DMEM for 1 h. Firstly, the supernatant was discarded, and the cells were washed once with fresh DMEM. Then the medium was replaced with fresh DMEM containing 2% FBS. For titer detection of SVCV, the viral supernatant to be tested was serially diluted 10 times in DMEM. Subsequently, each dilution was used to infect 3 duplicate holes of EPC cells in 48-well plate. After three days post-infection, the viral plaques were counted. Besides, the virus production method was as previously described (He et al., 2023). Briefly, the EPC cells in 10 cm plates were infected with SVCV at a low MOI by using the infection methods mentioned above. When the cytopathic effect (CPE) reached approximately 50%, the supernatant was collected and filtered through a 0.22 μ m filter. Finally, the filtered supernatant was aliquoted and stored at $-80\,^{\circ}$ C.

2.3. Luciferase reporter assay

The EPC cells seeded in 24-well plate were co-transfected with pRL-TK (50 ng), and either Luci- $bcIFN\alpha$, Luci- $DrIFN\phi$ 1, or Luci-epcIFN (200 ng) and plasmids expressing bcHSC70. The PLB-lysed cells were used to measure the activities of firefly luciferase and renilla luciferase as previously (He et al., 2023).

2.4. Immunoblotting (IB)

The immunoblotting assay as previously described (Yang et al., 2023). Briefly, the transfected HEK293T or EPC cells were harvested at 48 h post-transfection (hpt) and the cell lysates were collected with 1 % NP40 buffer, then boiled in 5 \times SDS-PAGE Loading Buffer (NCM Biotech, China) for 5–10 min. The proteins in the lysates were separated by SDS-PAGE gels and then transferred to a PVDF membrane (Millipore, USA). The membranes were probed with mouse anti-HA/Flag/Myc monoclonal antibody (1:5000, Abmart, China) overnight at 4 $^{\circ}$ C and were incubated with goat-anti-mouse IgG secondary antibody (1:30000, Sigma, USA). Finally, the BCIP/NBT Alkaline Phosphatase Color Development Kit (Thermo, USA) was used to visualize the specific protein bands.

2.5. Co-immunoprecipitation (co-IP)

HEK293T cells were co-transfected with the relative plasmids and those cells were harvested and lysed after 48 hpt for Co-

Table 1
Primers used in the study.

Primer name	Sequence (5′–3′)	Primer information
CDS		
bcHSC70-F	ATGTCCAAGGGACCAGCTG	For bcHSC70 CDS cloning
bcHSC70-R	TTAGTCGACCTCCTCGATG	
Expression vector		
bcHSC70-N-F	ACTGACGGTACCATGTCCAAGGGACCAG	For expression vector construction
bcHSC70-N-R	ACTGACCTCGAGTTAGTCGACCTCCTCG	
bcHSC70-C-F	ACTGACGGTACCGCCACCATGTCCAAGGGACC	
bcHSC70-C-R	ACTGACCTCGAGGTCGACCTCCTCGATG	
qRT-PCR		
Q-bcactin-F	TGGGCACCGCTTCCT	
Q-bcactin-R	TGTCCGTCAGGCAGCTCAT	
Q-HSC70-F	GTCGCTATGAACCCCACCAA	
Q-HSC70-R	TGGGACGGTATTGTCGTTG	
Q-bcMX1-F	TGAGCGTAGGCATTAGCAC	
Q-bcMX1-R	CCTGGAGCAGATAGCG	
Q-bcPKR-F	GAGCGGACTAAAAGGACAGG	
Q-bcPKR-R	AAAATATATGAGACCCAGGG	
Q-bcViperin-F	CCAAAGAGCAGAAAGAGGGACC	
Q-bcViperin-R	TCAATAGGCAAGACGAACGAGG	
Q-SVCV-G-F	GATGACTGGGAGTTAGATGGC	
Q-SVCV-G-R	ATGAGGGATAATATCGGCTTG	
Q-SVCV-M-F	CGACCGCCCAGTATTGATGGATAC	
Q-SVCV-M-R	ACAAGGCCGACCCGTCAACAGAG	
Q-SVCV-N-F	GGTGCGAGTAGAAGACATCCCCG	
Q-SVCV-N-R	GTAATTCCCATCATTGCCCCAGAC	
Q-SVCV-P-F	AACAGGTATCGACTATGGAAGAGC	
Q-SVCV-P-R	GATTCCTCTTCCCAATTGACTGTC	
shRNA		
sh-1-bcHSC70-F	CCGGGGACAAGCAGAAGATCCTTGACTCGAGTCAAGGATCTTCTGCTTGTCCTTTTTTG	
sh-1-bcHSC70-R	AATTCAAAAAGGACAAGCAGAAGATCCTTGACTCGAGTCAAGGATCTTCTGCTTGTCC	
sh-2-bcHSC70-F	CCGGGCACCTTCGATGTCTATCCCTCGAGGGATAGACACATCGAAGGTGCTTTTTG	
sh-2-bcHSC70-R	AATTCAAAAAGCACCTTCGATGTGTCTATCCCTCGAGGGATAGACACATCGAAGGTGC	
sh-3-bcHSC70-F	CCGGGGACAAGGCTCAGATCCATGACTCGAGTCATGGATCTGAGCCTTGTCCTTTTTG	
sh-3-bcHSC70-R	AATTCAAAAAGGACAAGGCTCAGATCCATGACTCGAGTCATGGATCTGAGCCTTGTCC	

immunoprecipitation (co-IP) assay as previously described (Liu et al., 2024). In short, the whole-cell lysates were incubated with protein A/G agarose beads (Sigma, USA) at 4 $^{\circ}$ C for 1 h. After centrifugation at 5000g for 2 min to remove the beads, the supernatant was transferred to anti-Flag/HA-conjugated protein A/G agarose beads (Sigma, USA) and incubated overnight at 4 $^{\circ}$ C for 4 h. And then the beads were washed 5 times with 1 $^{\circ}$ MP40 buffer and then heated-denatured in 5 $^{\times}$ SDS-sample buffer. Finally, the above samples were used for IB as above.

2.6. Quantitative real-time PCR (qRT-PCR)

The relative transcription level of *bcHSC70*, *bcPKR*, *bcMX1*, *bcViperin* and *SVCV-P*, *G*, *M*, *N* were examined by qRT-PCR using the Applied Biosystems QuantStudio 5 RealTime PCR Systems (Thermo, USA). Specifically, total RNA from EPC or MPK cells were extracted via the RNA rapid extraction kit (Magen, China), and the RNA were reverse-transcribed into cDNA by using reverse transcriptase (Takara, Japan); qRT-PCR was detected using the SYBR Green I (Vazyme, China); The qRT-PCR reactions were performed using a standard program: 1 cycle at 95 °C for 10 min, 40 cycles of 95 °C for 15 s and 60 °C for 1 min. The data were analyzed using the $2^{-\Delta\Delta CT}$ method and experiments were performed in triplicate to ensure data reliability. The primers were listed in Table 1.

2.7. Immunofluorescence microscopy (IF)

The HeLa cells were transfected with HA-bcHSC70 and/or bcRIG-I-Flag by using LipoMax. The cells were fixed with 4% paraformaldehyde (Solarbio, China) at 24 hpt. The fixed cells were treated 0.2% Triton X-100 and 10% FBS used for immune-fluorescent staining as previously described (Wei et al., 2024). Mouse monoclonal anti-Flag antibody (Abmart, China) or rabbit monoclonal anti-HA antibody

(Abmart, China) was probed at the ratio of 1:500; Alexa Fluor 488 (Thermo, USA) goat anti-mouse or Alexa Fluor 594 goat (Thermo, USA) anti-rabbit was probed at the ratio of 1:1000; The cell nucleus was stained with Hoechst 33342 (Solarbio, China) according to the manufacturer's instructions.

2.8. Statistics analysis

For the statistical analysis of the data in reporter assay qRT-PCR, reporter assay viral titration and qRT-PCR, viral titration, all data were obtained from three independent experiments with each performed in triplicate. Error bars represent the standard error of the mean across these three independent experiments. Asterisk (*) stands for $p < 0.05, \, (**)$ stands for p < 0.01.

3. Results

3.1. Sequence analysis of bcHSC70

To study the role of bcHSC70 in teleost, the cDNA of HSC70 was cloned from MPK cells and the coding sequence of bcHSC70 consists of 1950 nucleotides (NCBI accession number: PQ511126), which encodes 650 amino acids (Fig. 1A). The calculated molecular weight of bcHSC70 is 71 kDa and the theoretical isoelectric point of bcHSC70 is 5.31 by website (http://web.expasy.org/protparam/).

In order to explore the sequence conservation of HSC70 among different vertebrates, the HSC70 sequence of human, mouse, chicken, zebrafish, african clawed frog and black carp were aligned together using the ClustalW2 program and edited with GeneDoc software (Fig. 1A). The results revealed that HSC70 sequences are highly conserved across the vertebrates, exhibiting over 95% similarity. Notably, these sequences share consistent structural domains: an N-

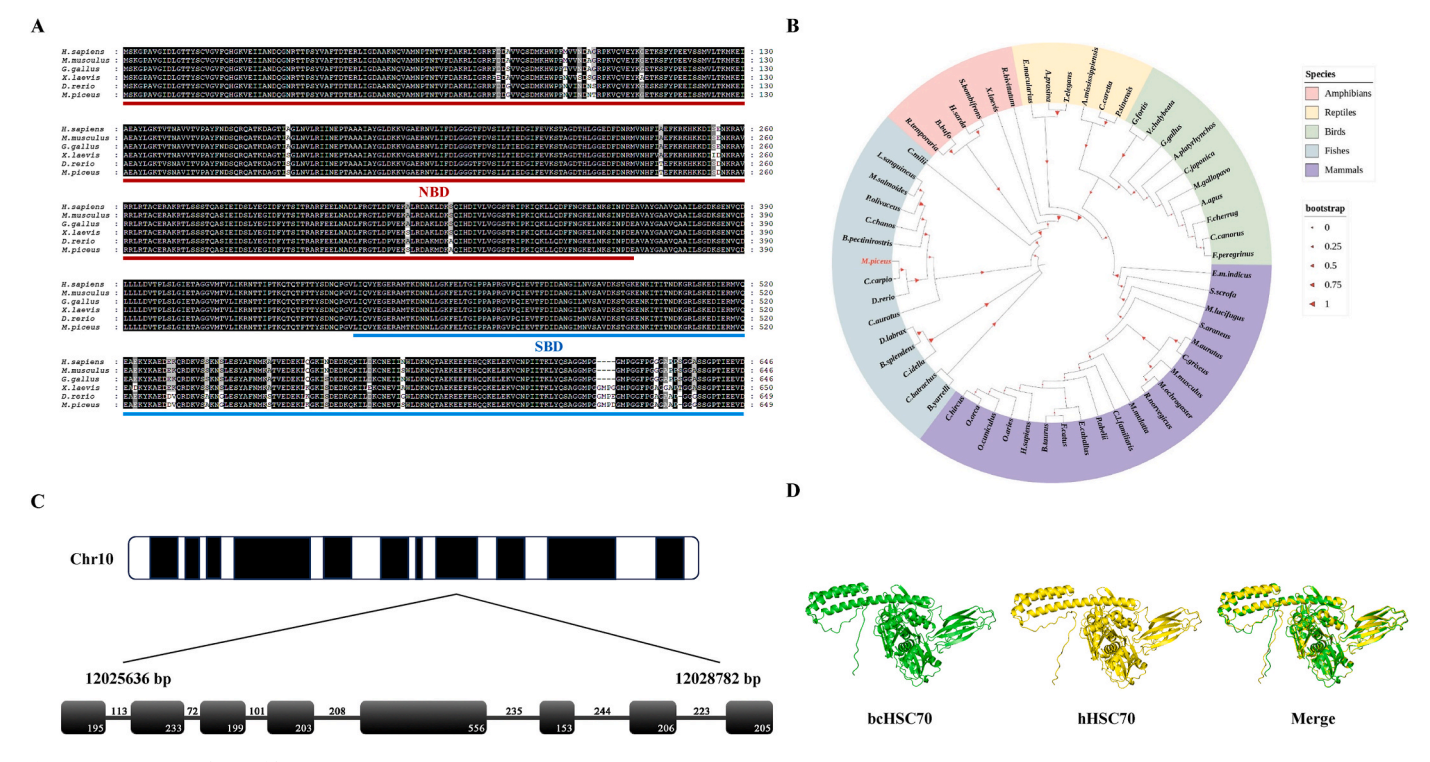


Fig. 1. Sequence analysis of bcHSC70

Amino acid sequence alignment analysis of bcHSC70 with HSC70 from *H. sapiens*, *M. musculus*, *G. gallus*, *D. rerio*, and *X. laevis* was conducted using MEGA7 and GeneDoc. The NBD and SBD domains of HSC70 were marked (A). A phylogenetic tree of HSC70 across vertebrates was constructed using the GeneDoc software and iTOL (https://itol.embl.de/) website. The NCBI accession numbers for the sequences used in the tree are listed in Table 2 (B). Three-dimensional structures of bcHSC70 and hHSC70 were constructed and compared via Swiss-model website (C). Transcriptome information was used to construct the localization of bcHSC70 on the chromosomes of black carp (D).

terminal nucleotide-binding domain (NBD) and a C-terminal substrate-binding domain (SBD). Then, to investigate the evolutionary process of HSC70, we constructed phylogenetic tree and multiple alignments based on the amino acid sequences of multiple species of HSC70 which were listed in Table 2, and categorized them according to mammals, birds, fishes, reptiles, and amphibians (Fig. 1B). The results indicated that bcHSC70 has the closest evolutionary relationship with zebrafish and common carp. Besides, we employed the SWISS-MODEL (https://swissmodel.expasy.org/) to predict and compare the 3D structures of bcHSC70 and human HSC70 (hHSC70), based on their amino acid sequences (Fig. 1D). The results revealed a high degree of structural similarity between the two proteins. Following this, utilizing the genome data of black carp, we pinpointed the location of bcHSC70 on chromosome 10 and it comprises 8 exons and 7 introns (Fig. 1C).

3.2. Protein expression and subcellular distribution of bcHSC70

In order to investigate the expression of bcHSC70 *in vitro*, HEK293T and EPC cells transfected with HA-bcHSC70 were harvested at 48 hpt and lysed cells were detected by IB assay. The results showed that bcHSC70 could normally express in both types of cells, and the expressed protein migrated at approximately 71 kDa, which was consistent with our predictions (Fig. 2A and B). Furthermore, to ascertain the distribution of bcHSC70, we overexpressed bcHSC70 in HeLa cells and the transfected cells were harvested at 24 hpt for IF staining. The results showed that the red color representing bcHSC70 expression area surrounded the nucleus (blue color). The above experimental results indicated that bcHSC70 was primarily localized in the cytoplasm (Fig. 2C).

3.3. Transcription activity of bcHSC70 in response to different stimuli

To clarify the expression pattern of bcHSC70 in response to different stimuli, we used qRT-PCR to examine the transcription levels of bcHSC70 in MPK cells after infection with SVCV (MOI = 0.1 or 0.01) and stimulation with Poly (I:C) (5 μ g/mL or 50 μ g/mL) or LPS (1 μ g/mL or 50 μ g/mL). After SVCV infection, when MOI = 0.1, the mRNA level of bcHSC70 initially reached its peak at 24h (1.5-fold), and ultimately dropped to the lowest point (0.3-fold). Similarly, when MOI = 0.01, the mRNA level of bcHSC70 within 12 h post-stimulation was up to highest (2.0-fold) and then fell to the lowest point at 48h (0.6-fold) (Fig. 3A). After Poly (I:C) treatment, the mRNA level of bcHSC70 rose to the highest point (5 µg/ml, 8.1-fold) at 12 h, and then showed a downward trend (Fig. 3B). In the LPS treatment group, the mRNA level of bcHSC70 increased to a maximum at 12 h (50 µg/mL, 73.0-fold) (Fig. 3C). The above results suggested that the expression of bcHSC70 in host cells after different stimuli showed the similar trend of first increasing and then decreasing, which indicated that bcHSC70 may be involved in the host innate immune response induced by viruses and bacteria.

3.4. bcHSC70 attenuated IFN signaling

The RLR/IFN signaling pathway plays a crucial role in the antiviral innate immunity in fish. Previous studies have confirmed that HSC70 interacts with MAVS in mammals, thereby exerting a negative regulatory effect on the RLR/IFN signaling pathway. To further elucidate the role of bcHSC70 in the RLR/IFN signaling pathway, we performed cotransfections of bcHSC70 with bcRIG-I/bcMDA5/bcMAVS/bcTBK1/bcIKK ϵ /bcIRF3/bcIRF7 in EPC cells, then used for reporter assay. The results indicated that bcHSC70 could inhibit the transcriptional activity of the *bcIFN* α promoter mediated by the above RLR factors (Fig. 4A), and the most obvious inhibitory effects were bcRIG-I and bcMAVS. However,

Table 2
Comparison of vertebrate HSC70 homologues (%).

Species	Similarity	Identity	Accession Number
Mammals:			
Homo sapiens	98	96	XP_054224589.1
Mus musculus	98	96	NP_112442.2
Rattus norvegicus	98	96	NP_077327.1
Bos taurus	98	96	NP_776770.2
Pongo abelii	98	96	NP_001125783.1
Cricetulus griseus	98	96	NP_001233658.1
Sorex araneus	98	96	XP_004604817.1
Myotis lucifugus	98	96	XP_006105485.1
Microtus ochrogaster	98	96	XP_005347192.1
Sus scrofa	98	96	NP_001230836.1
Mesocricetus auratus	99	97	XP_040586126.1
Equus caballus	98	96	NP_001075247.1
Ovis aries	98	96	XP_011951023.2
Capra hircus	98	95	AFN69444.1
Felis catus	98	96	XP_003992527.1
Oryctolagus cuniculus	98	96	XP_051715102.1
Macaca mulatta	98	96	NP_001248586.1
Orcinus orca	98	96	XP_004265984.2
Birds:			
Gallus gallus	98	96	NP_990334.2
Anas platyrhynchos	98	96	XP_027300025.1
Coturnix japonica	98	96	NP_001310129.1
Meleagris gallopavo	98	96	XP_003212746.1
Geospiza fortis	98	96	XP_005428927.1
Apus apus	98	96	XP_051494615.1
Falco cherrug	98	96	XP_055584512.1
Falco peregrinus	98	96	XP_005236669.1
Cuculus canorus	98	96	XP_053942910.1
Fishes:			
Danio rerio	99	99	NP_001103873.1
Ctenopharyngodon Idella	97	92	XP_051720133.1
Cyprinus carpio	99	99	XP_042588704.1
Clarias batrachus	97	92	AGO59146.1
Carassius auratus	99	97	XP_026082004.1
Lutjanus sanguineus	99	97	ADK88904.1
Dicentrarchus labrax	97	91	XP_051261532.1
Callorhinchus milii	98	94	NP_001279148.1
Micropterus salmoides	99	97	XP_038564876.1
Boleophthalmus pectinirostris	98	96	XP_020790269.1
Chanos chanos	99	99	XP_030647953.1
Bagarius yarrelli	98	95	TSK16160.1
Betta splendens	97	92	XP_028985702.1
Amphibians:			
Xenopus laevis	95	93	AAH41201.1
Spea bombifrons	98	96	XP_053323509.1
Hyla sarda	98	96	XP_056400669.1
Bufo bufo	98	95	XP_040286924.1
Rana temporaria	98	95	XP_040182323.1
Rhinatrema bivittatum	97	95	XP_029430042.1
Reptiles:			
Thamnophis elegans	98	95	XP_032085137.1
Pelodiscus sinensis	98	96	NP_001273837.1
Caretta caretta	98	96	XP_048683618.1
Eublepharis macularius			
Ediotopitas to macettas tao	98	96	XP_054854152.1

the regulatory role of HSC70 on RIG-I has not been studied extensively in teleost fish. To further investigate the regulatory role of bcHSC70 on bcRIG-I in the IFN signaling pathway, we co-transfected bcHSC70 and bcRIG-I into EPC cells for reporter assay, and the results showed that the bcRIG-I-mediated transcriptional activities of $bcIFN\alpha$, epcIFN and $DrIFN\varphi 1$ promoter were strongly inhibited by bcHSC70 (Fig. 4B–D). The above results implied that bcHSC70 exerts a negative regulatory effect in the RIG-I/IFN signaling pathway.

3.5. bcHSC70 down-regulated bcRIG-I-mediated antiviral ability

Our previous study has identified that overexpressed bcRIG-I could significantly enhance the ability of EPC cells to resist SVCV (Liu et al., 2023). To ascertain the role of bcHSC70 in the bcRIG-I-mediated innate

antiviral response, we co-transfected EPC cells with bcHSC70 and bcRIG-I, and then infected with SVCV at different MOIs (1 or 0.1). After 24 h, the supernatant was harvested for plaque assay, while the cell pellets were used for qRT-PCR. The plaque assay results indicated a significantly increase in viral titer in EPC cells co-transfected with bcRIG-I and bcHSC70 compared to those transfected solely with bcRIG-I, suggesting a potential inhibitory role of bcHSC70 on bcRIG-I-mediated antiviral activity (Fig. 5. A&B). Meanwhile, the transcription levels of SVCV-P, SVCV-G, SVCV-M and SVCV-N in the cells co-transfected with bcRIG-I and bcHSC70 were observably higher than those in the cells transfected with bcRIG-I solely (Fig. 5C). The above results clearly demonstrated that bcHSC70 restrained bcRIG-I-mediated antiviral response.

3.6. Knockdown of bcHSC70 potentiated host antiviral activity

To investigate the influence of bcHSC70 knockdown on host antiviral ability, we constructed three shRNA knockdown plasmids specifically targeting bcHSC70 (bcHSC70-sh1, bcHSC70-sh2 and bcHSC70-sh3) and assessed their knockdown efficiency in HEK293T cells using IB. The results indicated that bcHSC70-sh3 significantly reduced the expression level of exogenous bcHSC70 (Fig. 6A). Additionally, qRT-PCR results showed that bcHSC70-sh3 also restrained the transcriptional activity of HSC70 in MPK cells (Fig. 6B). Whereafter, MPK cells were transfected with bcHSC70-sh3 or scramble as a negative control, and then infected with SVCV (MOI = 0.1). The supernatant was collected after 24 h for SVCV titration, while the cells were harvested for qRT-PCR analysis. The result showed that the virus titer in the bcHSC70 knockdown group was lower than that in the control group (Fig. 6C). Moreover, the mRNA transcriptional levels of host genes including bcViperin, bcMx1 and bcPKR in the bcHSC70 knockdown group were dramatically enhanced than those in the control group (Fig. 6D). Additionally, the mRNA expression levels of SVCV genes (SVCV-P, SVCV-G, SVCV-M, and SVCV-N) were markedly reduced in MPK cells transfected with bcHSC70-sh3 (Fig. 6E). These results demonstrate that the knockdown of bcHSC70 promotes host cellular antiviral activity.

3.7. The interaction between bcHSC70 and bcRIG-I

In order to examine the interaction between bcHSC70 and bcRIG-I, HA-bcHSC70 and bcRIG-I-Flag were co-transfected into HEK293T cells for subsequent co-IP assay. The co-IP experiments revealed that specific bands of HA-bcHSC70 could be detected in the precipitates of bcRIG-I-Flag. Similarly, the specific bands of bcRIG-I-Flag could be detected in the precipitates of HA-bcHSC70, which demonstrated the direct interaction between these two proteins (Fig. 7A and B). Furthermore, HeLa cells were co-transfected with bcHSC70 and bcRIG-I and used for IF assay, and the IF data clearly showed overlapping regions between green fluorescence (representing bcRIG-I) and red fluorescence (representing bcHSC70), indicating that these two proteins have consistent subcellular distributions (Fig. 7C). These results indicate that bcHSC70 interacts with bcRIG-I.

3.8. bcHSC70 decreased the K63-linked ubiquitination of bcRIG-I

Previous studies have shown that K63-linked ubiquitination of RIG-I were required to activate downstream signaling transduction, while the RIG-I stability were regulated by K48-linked ubiquitination (Madiraju et al., 2022; Tracz et al., 2021). To explore whether bcHSC70 regulates the activity of bcRIG-I through affecting its ubiquitination, we co-transfected Myc-Ub, bcRIG-I-Flag, and/or HA-bcHSC70 into HEK293T cells and conducted co-IP experiments. The results indicated that bcHSC70 could reduce the overall ubiquitination level of bcRIG-I (Fig. 8A). To further confirm the type of polyubiquitin chains on bcRIG-I in the presence of bcHSC70, the HEK293T cells were co-transfected HA-Ub/K63O/K48O, bcRIG-I-Flag, and/or

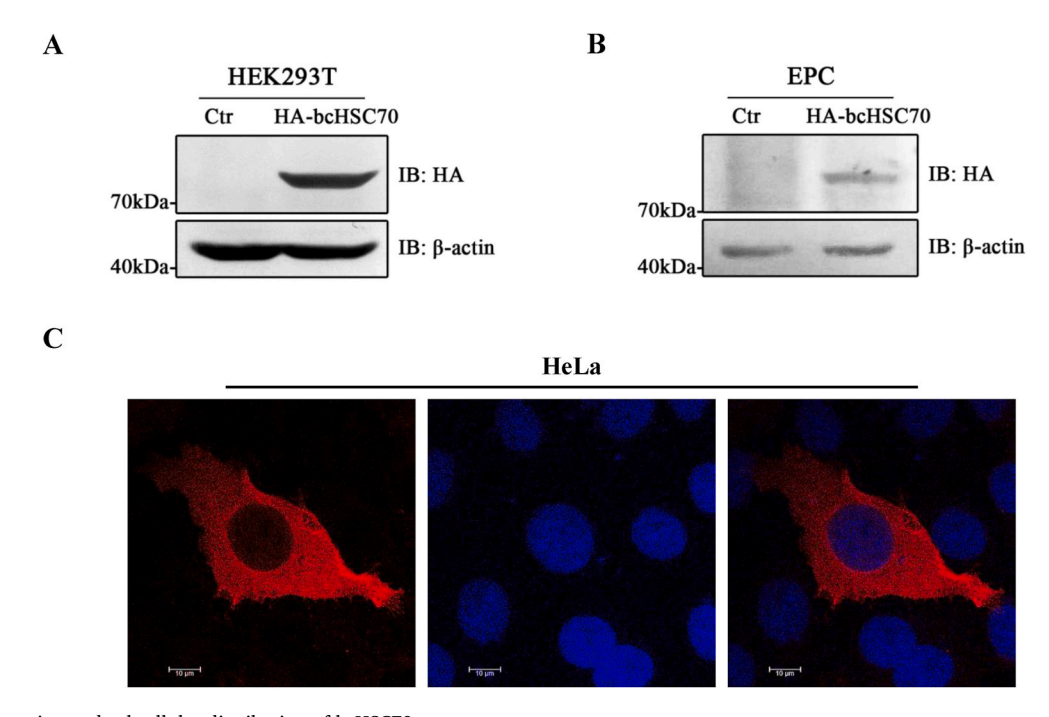


Fig. 2. Protein expression and subcellular distribution of bcHSC70 HEK293T (A) or EPC (B) cells were transfected with 3 μg of bcHSC70 recombinant plasmid or pcDNA5/FRT/TO plasmid, respectively. At 48 hpt, the cells were harvested and lysed for IB. Additionally, HeLa cells in 24-well plates were transfected with 500 ng of bcHSC70 using LipoMax. At 48 hpt, these transfected HeLa cells were used for IF staining (C). The scale bars in (C) represent 10 μm (μm). HA-bcHSC70: pcDNA5/FRT/TO-HA-bcHSC70; Ctr: pcDNA5/FRT/TO.

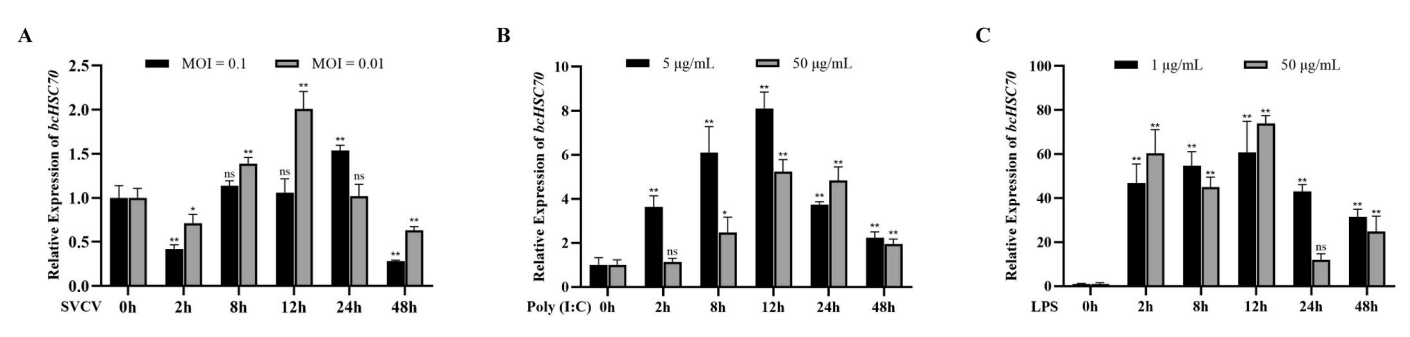


Fig. 3. mRNA expression patterns of bcHSC70 in response to different stimuli The mRNA levels of bcHSC70 were detected in MPK cells at different time points (0h, 2h, 8h, 12h, 24h and/or 48h) after stimulation with: SVCV at an MOI of 0.1 or 0.01 (A); Poly (I:C) at concentrations of 5 μ g/mL or 50 μ g/mL (B); LPS at concentrations of 1 μ g/mL or 50 μ g/mL (C). The experiments were performed in triplicate to ensure data reliability. *p < 0.05, **p < 0.01.

bcHSC70-Myc, respectively. The co-IP and gray ratio analysis results revealed that bcHSC70 significantly reduced the K63-linked ubiquitination of bcRIG-I (approximately a 44% decrease) but not the K48-linked ubiquitination (Fig. 8B). These results suggested that HSC70 negatively regulated IFN signaling by decreasing K63-linked ubiquitination of RIG-I in black carp.

4. Discussion

Heat shock cognate 70 (HSC70) belongs to the HSP70 protein family (Zininga et al., 2018), which is highly conserved across distinct species and shares similar domain structures, including the N-terminal nucleotide-binding domain (NBD) and the C-terminal substrate-binding domain (SBD) (Silva et al., 2021). Specifically, the NBD domain, which has a size of 44 kDa, consists of four residues: Ia, Ib, IIa, and IIb. The SBD is made up of two subdomains: a 15 kDa β -sandwich domain that binds peptide substrates and a 10 kDa R-helix domain that serves as the substrate-binding site (Stricher et al., 2013). In this study, we successfully cloned the HSC70 homolog from black carp (bcHSC70) and

analyzed its conservation with other vertebrate species. The results showed that bcHSC70 exhibits a remarkably high degree of conservation across varied species, and possesses the same structural domains, such as the NBD and SBD domains (Fig. 1A). Previous research has showed that variations in these domains determine the specificity of HSC70 in binding substrates and its functional diversity (Stricher et al., 2013; Wang et al., 2020). Notably, the G/P-rich terminal region within the SBD of bcHSC70 is less conserved compared to HSC70 from other species. This may be one of the reasons why bcHSC70 targets the substrate RIG-I and regulates its mediated antiviral response in black carp, but the concrete mechanism remains to be further studied.

Recent studies have indicated that HSC70 plays different regulatory roles in different viral infections. For example, HSC70 has been identified as a positive regulator of human hepatitis B virus (HBV) replication (Wang et al., 2023), however, it can also restrict dengue virus (DENV) replication (Vega-Almeida et al., 2013). In this study, we found that the knockdown of bcHSC70 could enhance cellular antiviral signaling and overexpressed bcHSC70 could weaken bcRIG-I-mediated IFN expression and antiviral activity. However, recent studies have shown that HSC70

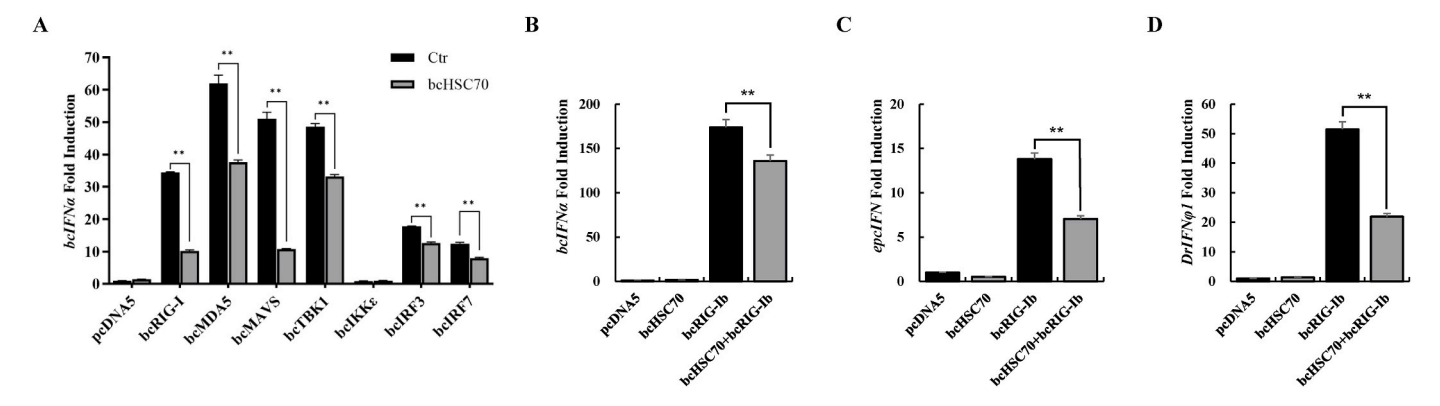


Fig. 4. bcHSC70 inhibits bcRIG-I-mediated IFN promoter transcription Each of the plasmids bcRIG-I, bcMDA5, bcMAVS, bcTBK1, bcIKKε, bcIRF3 and bcIRF7 was co-transfected with pRL-TK, Luci-bcIFNα and/or bcHSC70 into EPC cells, respectively, and then cells were lysed with passive lysis buffer (PLB) and were used for luciferase report assay at 24 hpt. EPC cells in 24-well plates were transfected with bcRIG-I and/or bcHSC70, pRL-TK, and different IFN promoter plasmids (Luci-bcIFNα (B), Luci-epcIFN(C) and Luci-DrIFN φ 1(D)), and then these cells were used for luciferase report assay as described above. The total amount of plasmid DNA in each well was balanced by the addition of empty vectors. The experiments were performed in triplicate to ensure data reliability. *p < 0.05, **p < 0.01.

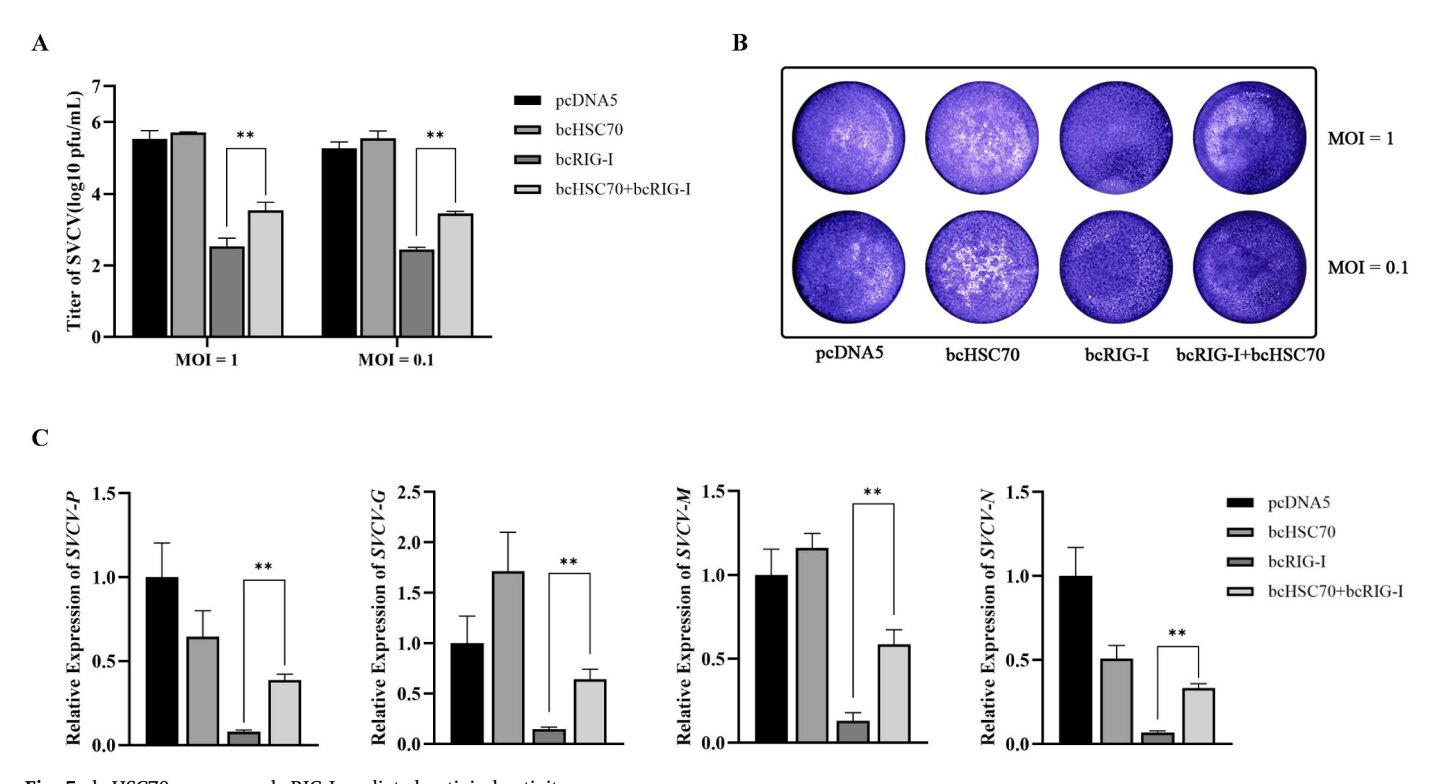


Fig. 5. bcHSC70 suppresses bcRIG-I-mediated antiviral activity EPC cells in 24-well plate were transfected with 250 ng bcHSC70, 250 ng bcRIG-I and/or bcHSC70 respectively. The transfected cells were infected with SVCV (MOI = 0.1 or 1). At 24 h post-infection: The supernatant was collected for virus titer assay (A). The monolayer cells were stained with crystal violet for visualization of cell viability and morphological changes (B). Additionally, using the same transfection system as described for (A), then these transfected cells were infected with SVCV at an MOI of 1. At 24 h post-infection, the monolayer cells were collected for qRT-PCR analysis to determine the relative mRNA levels of SVCV-P, G, M, N (C). The experiments were performed in triplicate to ensure data reliability. *p < 0.05, **p < 0.01.

could inhibit SVCV replication by promoting G protein degradation in zebrafish (Li et al., 2021), which was inconsistent with our experimental results. Other genes have similar regulatory mechanisms in teleost, such as the LGP2 in rainbow trout, which promotes the IFN production to against Viral hemorrhagic septicemia virus (VHSV) infection. (Chang et al., 2011); Conversely, the overexpressed LGP2 could reduce the transcriptional level of IFN and antiviral genes in orange-spotted grouper, thereby enhancing susceptibility to red-spotted grouper nervous necrosis virus (RGNNV) (Yu et al., 2016); Therefore, HSC70 might also play distinct roles in different fish species or tissues, revealing the functional diversity of bcHSC70 in innate immunity.

Ubiquitination is one of the crucial post-translational modification (PTM) of proteins that can affect their stability, interactions, and biological functions (Rennie et al., 2020). Differences in the types of ubiquitin chains have distinct functions in the RLR signaling pathway. For instance, RIG-I is targeted for K63-linked ubiquitination by multiple regulators including CYLD, USP21, and USP3, regulating IRF3 phosphorylation and IFN production (Cui et al., 2014; Oshiumi, 2020). Besides, K48-linked ubiquitination of RIG-I by multiple E3 ligases, such as RNF125/122, TRIM40 and CHIP, which leading to RIG-I degradation and attenuating IFN signaling (Chang et al., 2023; Wang et al., 2016; Zhao et al., 2016, 2017). Recent studies have shown that STAT2

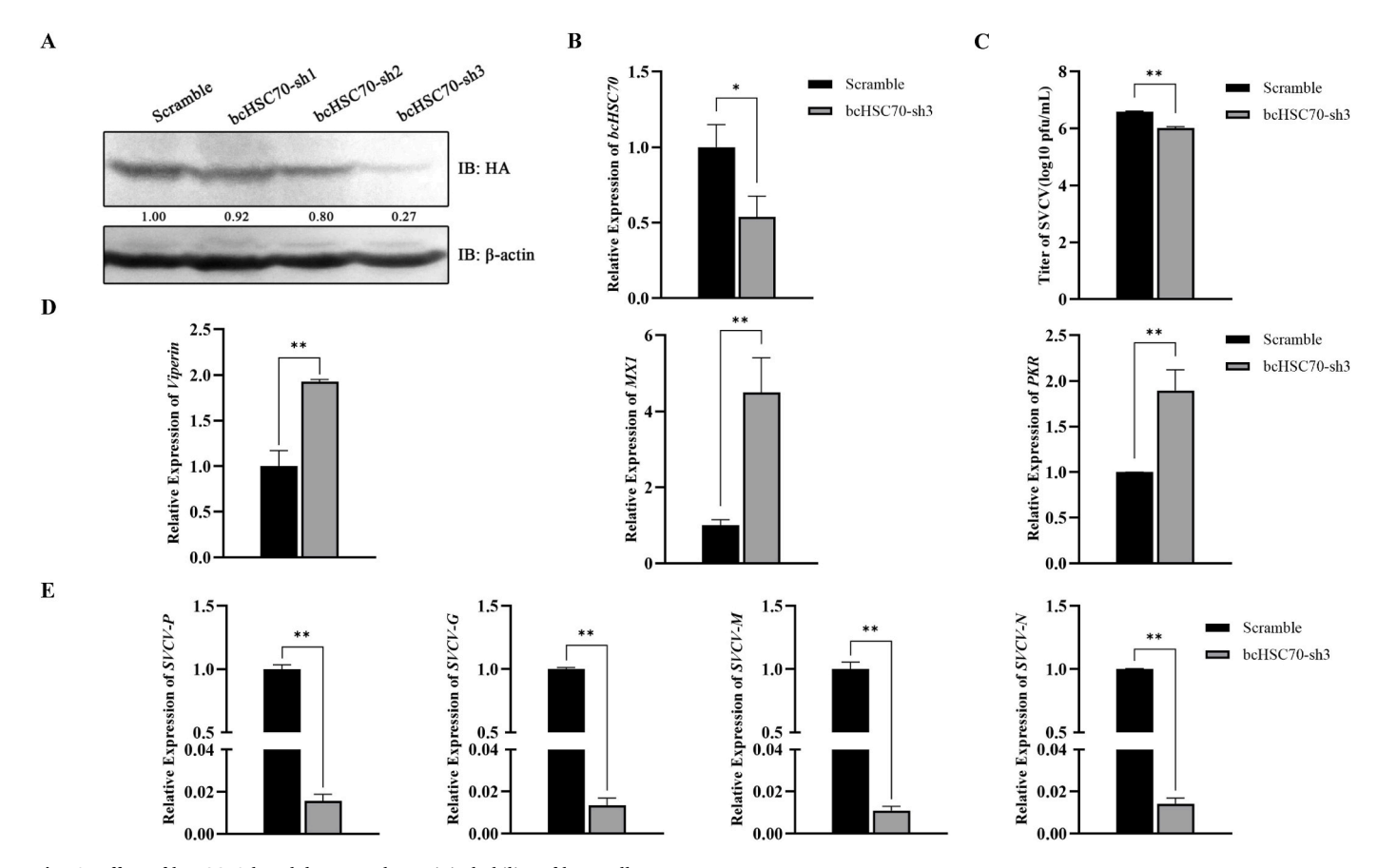


Fig. 6. Effect of bcHSC70 knockdown on the antiviral ability of host cells The HEK293T in 6-well plate were co-transfected with 1 μg pcDNA5-FRT/TO-HA-bcHSC70 and 2 μg pLKO.1-bcHSC70-shRNA (1, 2, 3) or pLKO.1-scramble-shRNA and the knockdown efficiency was detected by IB assay. The figure shows the gray ratio of the protein band of HA-bcHSC70 to the corresponding β-actin protein band. The gray value was calculated by Image J software (A). pLKO.1-bcHSC70-shRNA-3 or pLKO.1-scramble-shRNA plasmid were transfected into MPK cells, and the transcription level of bcHSC70 was detected by qRT-PCR after 24 hpt (B). Using the same transfection system as in (B), after 24 hpt, the transfected cells were infected by SVCV at an MOI of 0.1 for 24 h, and the supernatant was collected 24 h post-infection for virus titer assay (C), while monolayer cells were collected for qRT-PCR analysis to determine the relative mRNA levels of bcViperin, bcMX1, bcPKR (D), and SVCV-P, G, M, N (E). The experiments were performed in triplicate to ensure data reliability. *p < 0.05, **p < 0.01.

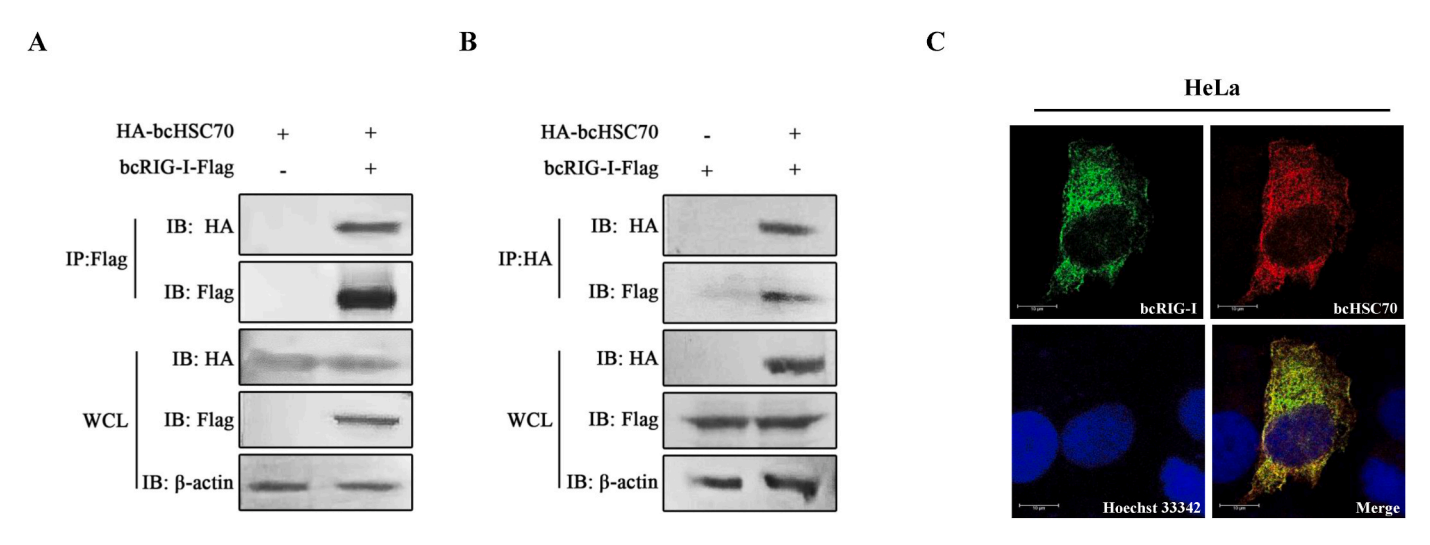
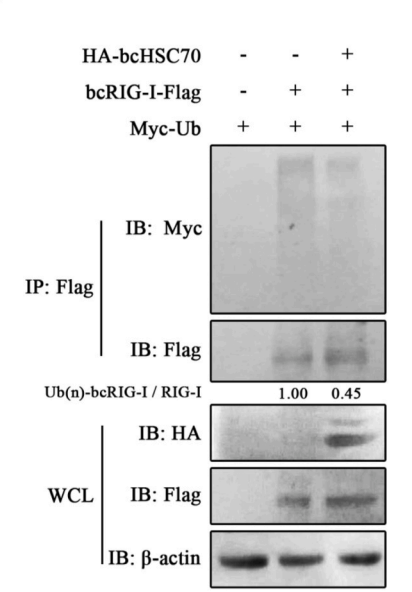


Fig. 7. Analysis of interaction between bcHSC70 and bcRIG-I HEK293T cells in 10 cm plates were co-transfected with 7.5 μ g of HA-bcHSC70 and/or 7.5 μ g of bcRIG-I-Flag (A) or 7.5 μ g of bcRIG-I-Flag and/or 7.5 μ g HA-bcHSC70 (B). The total amount of plasmid for each transfection was balanced with pcDNA5/FRT/TO. The transfected cells were harvested for co-IP. IP: Immunoprecipitation; IB: Immunoblot; WCL: Whole cell lysate. HeLa cells in 24-well plate were transfected with 250 ng of bcRIG-I-Flag and 250 ng of HA-bcHSC70 used for immunofluorescence experiments after 24 hpt. The scale bars represent 10 μ m (μ m) (C).

A



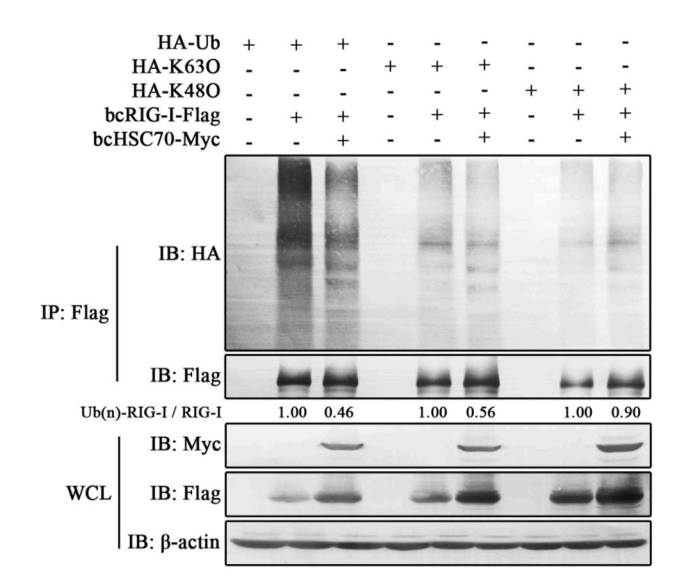


Fig. 8. bcHSC70 decreased K63-linked ubiquitination of bcRIG-I HEK293T cells were transfected with Myc-Ub, bcRIG-I-Flag and/or HA-bcHSC70. The transfected cells were harvested for co-IP at 48 hpt (A). HEK293T cells were transfected with HA-Ub/K63O/K48O, bcRIG-I-Flag and/or bcHSC70-Myc. The transfected cells were harvested for co-IP at 48 hpt (B).

B

inhibited K63-linked ubiquitination of RIG-I and negatively regulated its mediated IFN signaling pathway in black carp (Liu et al., 2024). In this article, our results showed that HSC70 could target RIG-I and weaken its K63-linked ubiquitination, negatively regulating RLR/IFN expression and antiviral activity in black carp. Generally, the K63 ubiquitin of RIG-I is mainly associated with its activation (Oshiumi, 2020). We speculate that the ubiquitination of RIG-I may be related to its activity in black carp, which is consistent with studies in mammals, suggesting that bcHSC70 can inhibit bcRIG-I activity by impacting its ubiquitination, thereby negatively regulating the RLR/IFN signaling pathway.

In conclusion, this study is the first to explore the negative regulatory mechanism of HSC70 within the RLR/IFN pathway in teleost fish. Our findings suggest that HSC70 inhibits RIG-I mediated antiviral response by weakening its K63-linked ubiquitination in black carp, which provides an important basis for studying the innate immune regulatory mechanisms in teleost fish.

CRediT authorship contribution statement

Jiaxin Fu: Writing – original draft, Investigation, Conceptualization. Nianfeng chen: Methodology, Investigation, Data curation. Tian Qin: Visualization, Validation. Yixin Chen: Visualization, Validation. Ji Liu: Writing – review & editing, Formal analysis. Hui Wu: Validation, Formal analysis. Jun Yan: Writing – review & editing, Visualization, Formal analysis. Jun Xiao: Validation, Investigation. Jun Zou: Writing – review & editing. Hao Feng: Supervision, Resources, Conceptualization.

Declaration of competing interest

The authors declare that they have no known competing financial interests or personal relationships that could have appeared to influence the work reported in this paper.

Acknowledgements

This work was supported the National Natural Science Foundation of China (U21A20268, U22A20535, U23A20252, 32173010, 32303050, 32002383), Hunan Provincial Science and Technology Department

(2023JJ10028), the Earmarked Fund for Hunan Agriculture Research System (HARS-07), Hunan Provincial education Department (20A317), the Research and Development Platform of Fish Disease and Vaccine for Post-graduates in Hunan Province.

Data availability

Data will be made available on request.

References

Bonam, S.R., Ruff, M., Muller, S., 2019. HSPA8/HSC70 in immune disorders: a molecular rheostat that adjusts chaperone-mediated autophagy substrates. Cells 8 (8), 849. https://doi.org/10.3390/cells8080849.

Chang, H., Hou, P., Wang, X., Xiang, A., Wu, H., Qi, W., Yang, R., Wang, X., Li, X., He, W., Zhao, G., Sun, W., Wang, T., He, D.C., Wang, H., Gao, Y., He, H., 2023. CD97 negatively regulates the innate immune response against RNA viruses by promoting RNF125-mediated RIG-I degradation. Cell. Mol. Immunol. 20 (12), 1457–1471. https://doi.org/10.1038/e41423-023-01103-7

Chang, M., Collet, B., Nie, P., Lester, K., Campbell, S., Secombes, C.J., Zou, J., 2011. Expression and functional characterization of the RIG-I-like receptors MDA5 and LGP2 in rainbow trout (Oncorhynchus mykiss). J. Virol. 85 (16), 8403–8412. https://doi.org/10.1128/JVI.00445-10.

Cui, J., Song, Y., Li, Y., Zhu, Q., Tan, P., Qin, Y., Wang, H.Y., Wang, R.-F., 2014. USP3 inhibits type I interferon signaling by deubiquitinating RIG-I-like receptors. Cell Res. 24 (4). https://doi.org/10.1038/cr.2013.170. Article 4.

Freed, E.O., Gale, M., 2014. Antiviral innate immunity: editorial overview. J. Mol. Biol. 426 (6), 1129–1132. https://doi.org/10.1016/j.jmb.2014.01.005.

Gomes, M.C., Mostowy, S., 2020. The case for modeling human infection in zebrafish. Trends Microbiol. 28 (1), 10–18. https://doi.org/10.1016/j.tim.2019.08.005.

Gong, X.-Y., Zhang, Q.-M., Gui, J.-F., Zhang, Y.-B., 2019. SVCV infection triggers fish IFN response through RLR signaling pathway. Fish Shellfish Immunol. 86, 1058–1063. https://doi.org/10.1016/j.fsi.2018.12.063.

He, Y., Liu, J., Miao, Y., Liu, M., Wu, H., Xiao, J., Feng, H., 2023. Black carp LGP2 suppresses RIG-I mediated IFN signaling during the antiviral innate immunity. Fish Shellfish Immunol. 143, 109208. https://doi.org/10.1016/j.fsi.2023.109208.

Jin, Y., Jia, K., Zhang, W., Xiang, Y., Jia, P., Liu, W., Yi, M., 2019. Zebrafish TRIM25 promotes innate immune response to RGNNV infection by targeting 2CARD and RD regions of RIG-I for K63-linked ubiquitination. Front. Immunol. 10, 2805. https://doi.org/10.3389/fimmu.2019.02805.

Kato, H., Fujita, T., 2015. RIG-I-like receptors and autoimmune diseases. Curr. Opin. Immunol. 37, 40–45. https://doi.org/10.1016/j.coi.2015.10.002.

Kowalinski, E., Lunardi, T., McCarthy, A.A., Louber, J., Brunel, J., Grigorov, B., Gerlier, D., Cusack, S., 2011. Structural basis for the activation of innate immune pattern-recognition receptor RIG-I by viral RNA. Cell 147 (2), 423–435. https://doi. org/10.1016/j.cell.2011.09.039.

Lai, Y., Liang, M., Hu, L., Zeng, Z., Lin, H., Yi, G., Li, M., Liu, Z., 2019. RNF135 is a positive regulator of IFN expression and involved in RIG-I signaling pathway by

- targeting RIG-I. Fish Shellfish Immunol. 86, 474–479. https://doi.org/10.1016/j.
- Leung, D.W., Amarasinghe, G.K., 2012. Structural insights into RNA recognition and activation of RIG-I-like receptors. Curr. Opin. Struct. Biol. 22 (3), 297–303. https:// doi.org/10.1016/j.sbi.2012.03.011.
- Li, C., Shi, L., Gao, Y., Lu, Y., Ye, J., Liu, X., 2021. HSC70 inhibits spring viremia of carp virus replication by inducing MARCH8-mediated lysosomal degradation of G protein. Front. Immunol. 12, 724403. https://doi.org/10.3389/ fimmu.2021.724403.
- Liao, Z., Su, J., 2021. Progresses on three pattern recognition receptor families (TLRs, RLRs and NLRs) in teleost. Dev. Comp. Immunol. 122, 104131. https://doi.org/10.1016/j.dci.2021.104131.
- Liu, J., Dai, C., Yin, L., Yang, X., Yan, J., Liu, M., Wu, H., Xiao, J., Kong, W., Xu, Z., Feng, H., 2024. STAT2 negatively regulates RIG-I in the antiviral innate immunity of black carp. Fish Shellfish Immunol. 148, 109510. https://doi.org/10.1016/j. fsi 2024 109510
- Liu, J., He, Y., Miao, Y., Dai, C., Yan, J., Liu, M., Zou, J., Feng, H., 2023. The phenylalanine-28 is crucial for black carp RIG-I mediated antiviral signaling. Dev. Comp. Immunol. 148, 104917. https://doi.org/10.1016/j.dci.2023.104917.
- Liu, Z., Wu, S.-W., Lei, C.-Q., Zhou, Q., Li, S., Shu, H.-B., Wang, Y.-Y., 2013. Heat shock cognate 71 (HSC71) regulates cellular antiviral response by impairing formation of VISA aggregates. Protein & Cell 4 (5), 373–382. https://doi.org/10.1007/s13238-013.33002.3
- Madiraju, C., Novack, J.P., Reed, J.C., Matsuzawa, S., 2022. K63 ubiquitination in immune signaling. Trends Immunol. 43 (2), 148–162. https://doi.org/10.1016/j. it 2021.12.005
- Oshiumi, H., 2020. Recent advances and contradictions in the study of the individual roles of ubiquitin ligases that regulate RIG-I-like receptor-mediated antiviral innate immune responses. Front. Immunol. 11. https://doi.org/10.3389/fimmu.2020.01296.
- Rennie, M.L., Chaugule, V.K., Walden, H., 2020. Modes of allosteric regulation of the ubiquitination machinery. Curr. Opin. Struct. Biol. 62, 189–196. https://doi.org/ 10.1016/j.sbi.2020.02.003.
- Silva, N.S.M., Rodrigues, L.F.D.C., Dores-Silva, P.R., Montanari, C.A., Ramos, C.H.I., Barbosa, L.R.S., Borges, J.C., 2021. Structural, thermodynamic and functional studies of human 71 kDa heat shock cognate protein (HSPA8/hHsc70). Biochimica et Biophysica Acta (BBA) - Proteins and Proteomics 1869 (12), 140719. https://doi. org/10.1016/j.bbapap.2021.140719.
- Solstad, A., Hogaboam, O., Forero, A., Hemann, E.A., 2022. RIG-I-like receptor regulation of immune cell function and therapeutic implications. J. Immunol. 209 (5), 845–854. https://doi.org/10.4049/jimmunol.2200395.
- Stricher, F., Macri, C., Ruff, M., Muller, S., 2013. HSPA8/HSC70 chaperone protein: structure, function, and chemical targeting. Autophagy 9 (12), 1937–1954. https://doi.org/10.4161/auto.26448.
- Thoresen, D., Wang, W., Galls, D., Guo, R., Xu, L., Pyle, A.M., 2021. The molecular mechanism of RIG-I activation and signaling. Immunol. Rev. 304 (1), 154–168. https://doi.org/10.1111/imr.13022.
- Tracz, M., Bialek, W., 2021. Beyond K48 and K63: non-canonical protein ubiquitination. Cell. Mol. Biol. Lett. 26 (1), 1. https://doi.org/10.1186/s11658-020-00245-6.

- Tutar, L., Tutar, Y., 2010. Heat shock proteins; an overview. Curr. Pharmaceut. Biotechnol. 11 (2), 216–222. https://doi.org/10.2174/138920110790909632.
- Vega-Almeida, T.O., Salas-Benito, M., De Nova-Ocampo, M.A., del Angel, R.M., Salas-Benito, J.S., 2013. Surface proteins of C6/36 cells involved in dengue virus 4 binding and entry. Arch. Virol. 158 (6), 1189–1207. https://doi.org/10.1007/s00705-012-1596-0
- Wang, W., Jiang, M., Liu, S., Zhang, S., Liu, W., Ma, Y., Zhang, L., Zhang, J., Cao, X., 2016. RNF122 suppresses antiviral type I interferon production by targeting RIG-I CARDs to mediate RIG-I degradation. Proc. Natl. Acad. Sci. USA 113 (34), 9581–9586. https://doi.org/10.1073/pnas.1604277113.
- Wang, Y., Zhao, M., Zhao, L., Geng, Y., Li, G., Chen, L., Yu, J., Yuan, H., Zhang, H., Yun, H., Yuan, Y., Wang, G., Feng, J., Xu, L., Wang, S., Hou, C., Yang, G., Zhang, N., Lu, W., Zhang, X., 2023. HBx-induced HSPA8 stimulates HBV replication and suppresses ferroptosis to support liver cancer progression. Cancer Res. 83 (7), 1048–1061. https://doi.org/10.1158/0008-5472.CAN-22-3169.
- Wang, Z., Li, Y., Yang, X., Zhao, J., Cheng, Y., Wang, J., 2020. Mechanism and complex roles of HSC70 in viral infections. Front. Microbiol. 11, 1577. https://doi.org/ 10.3389/fmicb.2020.01577.
- Wei, Y., Pei, S., Huang, Y., Yao, K., Yu, J., Yue, R., Wu, H., Xiao, J., Feng, H., 2024. UBE2J1 suppresses interferon signaling by facilitating the ubiquitination and degradation of IRF7. Aquaculture 595, 741640. https://doi.org/10.1016/j.aquaculture.2024.741640.
- Yang, C., Shu, J., Miao, Y., Liu, X., Zheng, T., Hou, R., Xiao, J., Feng, H., 2023. TRIM25 negatively regulates IKKe-mediated interferon signaling in black carp. Fish Shellfish Immunol. 142, 109095. https://doi.org/10.1016/j.fsi.2023.109095.
- Yang, G., Lee, H.E., Seok, J.K., Kang, H.C., Cho, Y.-Y., Lee, H.S., Lee, J.Y., 2021. RIG-I deficiency promotes obesity-induced insulin resistance. Pharmaceuticals 14 (11), 1178. https://doi.org/10.3390/ph14111178.
- Yang, X., Xie, L., Yin, Y., Yang, C., Xiao, J., Wu, H., Wang, C., Tian, Y., Feng, H., 2024.
 Black carp A20 inhibits interferon signaling through de-ubiquitinating IKKβ. Fish
 Shellfish Immunol. 152, 109781. https://doi.org/10.1016/j.fsi.2024.109781.
- Yu, Y., Huang, Y., Yang, Y., Wang, S., Yang, M., Huang, X., Qin, Q., 2016. Negative regulation of the antiviral response by grouper LGP2 against fish viruses. Fish Shellfish Immunol. 56, 358–366. https://doi.org/10.1016/j.fsi.2016.07.015.
- Zhao, C., Jia, M., Song, H., Yu, Z., Wang, W., Li, Q., Zhang, L., Zhao, W., Cao, X., 2017. The E3 ubiquitin ligase TRIM40 attenuates antiviral immune responses by targeting MDA5 and RIG-I. Cell Rep. 21 (6), 1613–1623. https://doi.org/10.1016/j.celrep.2017.10.020.
- Zhao, K., Zhang, Q., Li, X., Zhao, D., Liu, Y., Shen, Q., Yang, M., Wang, C., Li, N., Cao, X., 2016. Cytoplasmic STAT4 promotes antiviral type I IFN production by blocking CHIP-mediated degradation of RIG-I. J. Immunol. 196 (3), 1209–1217. https://doi. org/10.4049/jimmunol.1501224.
- Zininga, T., Ramatsui, L., Shonhai, A., 2018. Heat shock proteins as immunomodulants. Molecules 23 (11), 2846. https://doi.org/10.3390/molecules23112846.
- Zou, P.F., Chang, M.X., Li, Y., Huan Zhang, S., Fu, J.P., Chen, S.N., Nie, P., 2015. Higher antiviral response of RIG-I through enhancing RIG-I/MAVS-mediated signaling by its long insertion variant in zebrafish. Fish Shellfish Immunol. 43 (1), 13–24. https:// doi.org/10.1016/j.fsi.2014.12.001.